

DOI: <https://dx.doi.org/10.21123/bsj.2022.6924>

## Study the Nuclear Structure of Some Even-Even Ca Isotopes Using the Microscopic Theory

Tabarak Abdulla Alwan 

Ban Sabah Hameed\* 

Department of Physics, College of Science for Women, University of Baghdad, Baghdad, Iraq.

\*Corresponding author: [banalqazaz@yahoo.com](mailto:banalqazaz@yahoo.com)

E-mail addresses: [tabark.abdulla20@gmail.com](mailto:tabark.abdulla20@gmail.com)

Received 12/1/2022, Revised 4/3/2022, Accepted 6/3/2022, Published Online First 20/7/2022,  
Published 1/2/2023



This work is licensed under a [Creative Commons Attribution 4.0 International License](https://creativecommons.org/licenses/by/4.0/).

### Abstract:

The root-mean square-radius of proton, neutron, matter and charge radii, energy level, inelastic longitudinal form factors, reduced transition probability from the ground state to first-excited  $2^+$  state of even-even isotopes, quadrupole moments, quadrupole deformation parameter, and the occupation numbers for some calcium isotopes for  $A=42,44,46,48,50$  are computed using fp-model space and FPBM interaction.  $^{40}\text{Ca}$  nucleus is regarded as the inert core for all isotopes under this model space with valence nucleons are moving throughout the fp-shell model space involving  $1f_{7/2}$ ,  $2p_{3/2}$ ,  $1f_{5/2}$ , and  $2p_{1/2}$  orbits. Model space is used to present calculations using FPBM interaction, and with the effects of core-polarization are obtained by the first order core polarization through a microscopic theory is called modified surface delta interaction which allows all higher orbits are excited by particle-hole excitation from the core and model space orbits. Also, each isotope's effective charge is determined by using the collective model by Bohr and Mottelson formula. The current result corresponds to the experimental data by taking into account core polarization effects.

**Keywords:** Deformation parameters, Form factor, Occupation numbers, Quadrupole moments, Transition probability.

### Introduction:

Electron scattering ( $e,e$ ) is a good tool and sensitive to study the structure of stable and exotic nuclei, particularly neutron-rich nuclei. One of the most noteworthy features of exotic nuclei is that their electromagnetic properties, such as electric quadrupole moments (Q), quadrupole deformation parameters ( $\beta_2$ ), and reduced transition probability  $B(E2)\uparrow$ , can be examined theoretically and empirically. By single-particle configurations, all of these attributes convey information regarding nuclear structure<sup>1</sup>.

By permitting excitations from the core and model space orbits onto higher orbits, the electromagnetic properties can be added to the normal shell model treatment. Due to high-lying collective excitations, using first-order perturbation theory in the standard shell model configuration, core-polarization effects in electromagnetic and inelastic scattering transitions were observed, demonstrating a natural difference in neutron and proton polarization<sup>2</sup>.

The shell model is used by Ali<sup>3</sup> to compute effective charges of electric quadrupole transitions.

Theoretical results demonstrated that effective charges in light neutron-rich nuclei are good with the normal values.

Around the neutron number  $N=32$ , Garcia Ruiz et al<sup>4</sup> measured and calculated the electromagnetic properties of the ground-state like magnetic moments of  $^{49,51}\text{Ca}$  and quadrupole moments of  $^{47,49,51}\text{Ca}$ . The results for neutron-rich isotope moments agree very well with interactions predicted by chiral effective field theory, which includes three-nucleon forces.

According to theoretical conclusions<sup>5,6,7</sup> the shape in light neutron-rich nuclei implies decoupled quadrupole movements between protons and neutrons in those nuclei. A shell model with self-consistent Hartree-Fock computations has—been used by some researchers to examine the nuclear structure<sup>8</sup>. Some scholars have demonstrated the importance of transition probability  $B(E2)\uparrow$  values in nuclear physics study and model creation by examining the ratio of  $Z$  to  $N$  values, their relationship to nuclear magic numbers, and their growth along with the nuclear scheme<sup>9,10</sup>. In

general, the  $B(E2)\uparrow$  is affected by the scattering angle as well as the wave functions between the final and starting states<sup>11</sup>.

The nuclear structure is examined in this study for some calcium isotopes with  $A=42,44,46,48,50$  through electromagnetic transitions are calculated by adopting a shell model with the single-particle wave functions of the harmonic oscillator (HO), and using FPBM interaction<sup>12</sup> in the fp- shell model space. The nuclear shell model computations were done with the OXBASH shell model program<sup>13</sup>, which calculates the one-body density matrix (OBDM) elements in the spin-isospin formalism. The following calculations are compared to the values that were measured. Through effective charge, the core-polarization (CP) effects are included using the Bohr-Mottelson (B.M) formula, and obtained from a fit to spectroscopic data such as modified surface delta interaction (MSDI)<sup>14</sup>. The root-mean square-radius (rms) of proton, neutron, matter and charge radii, energy level, inelastic longitudinal form factors, reduced transition probability  $B(E2)\uparrow$ , quadrupole moment ( $Q$ ), quadrupole deformation parameters ( $\beta_2$ ) are computed, and the results are compared to the experimental data. Also, the occupation numbers (occ#) of the valence nucleons outside the  $^{40}\text{Ca}$  core are calculated to identify the contribution of these orbits for the valence nucleon.

### Theoretical framework

The electric transition operator  $\hat{E}_{JT}(\vec{r})$  for a system of  $k$  protons and neutrons identified using the isospin formalism, with the operator  $\hat{\tau}_z$ , such that  $\hat{\tau}_z|p\rangle = p$  for proton and  $\hat{\tau}_z|n\rangle = -n$  neutron and with  $e_{IS}$  and  $e_{IV}$  are the isoscalar and isovector charges, are provided by<sup>14</sup>.

$$\hat{E}_{JT}(\vec{r}) = \sum_{k=1}^n \left[ e_{IS} + e_{IV} \hat{\tau}_z \right] r_k^J Y_{JM}(\Omega_k), \quad \dots 1$$

Where  $r_k^J$  is the radial harmonic part and  $Y_{JM}(\Omega_k)$  is the spherical harmonic part.

The sum of the components of the one-body density matrix (OBDM) times the single-particle matrix elements are the reduced matrix element of the electric transition operator  $\hat{E}_{JT}$ , and is supplied by<sup>12</sup>:

$$\langle \Lambda_f || \hat{E}_{JT} || \Lambda_i \rangle = \sum_{j_f, j_i} OBDM(j_f, j_i, \Lambda_f, \Lambda_i)^{JT} \times \langle j_f t || \hat{E}_{JT} || j_i t \rangle \quad \dots 2$$

where states  $|\Lambda_i\rangle$  and  $|\Lambda_f\rangle$  are described the initial and final for the shell model-space wave functions

and  $j_f t$  and  $j_i t$  label single-particle states included the isospin.

The elastic and inelastic longitudinal form factors of electron scattering between initial and final states with multi polarity  $J$  and momentum transfer  $\vec{q}$  gave by<sup>15</sup>:

$$|F_{J^L}(q)|^2 = \frac{4\pi}{Z^2(2J_i + 1)} \left| \langle J_f || \hat{T}_{J^L}(q) || J_i \rangle \right|^2 |F_{c.m.}(q)|^2 \times |F_{f.s.}(q)|^2 \quad \dots 3$$

When,  $F_{f.s.}(q) = (1 + (\frac{q}{4.33})^2)^{-2}$  is the finite size form factors, and  $F_{c.m.}(q) = e^{\frac{q^2 b^2}{4A}}$  is the center of mass correction Form Factors in the shell model<sup>16,17</sup>.  $A$  is the mass number, and  $b$  is the harmonic oscillator (HO) size parameter.

One can be taken the core nucleons and the cut-out part of space consideration through a microscopic theory is called modified surface delta interaction (MSDI), then the wave functions and configurations with higher energy as first-order perturbation these are called the core polarization effects. The electric operator  $\hat{E}_{\Lambda}^{\eta}$ 's reduced matrix elements are stated as a sum of the model space (MS) and core polarization (CP) contributions, as shown below<sup>14</sup>:

$$\langle \Lambda_f || \hat{E}_{\Lambda}^{\eta} || \Lambda_i \rangle = \langle \Lambda_f || \hat{E}_{\Lambda}^{\eta} || \Lambda_i \rangle_{MS} + \langle \Lambda_f || \delta \hat{E}_{\Lambda}^{\eta} || \Lambda_i \rangle_{CP}, \quad \dots 4$$

The CP effects are computed to use the MSDI residual effective interaction.

$$\langle \Lambda_f || \delta \hat{E}_{\Lambda}^{\eta} || \Lambda_i \rangle_{CP} = \sum_{\alpha, \beta} \hat{X}_{\Lambda_f \Lambda_i}(\alpha, \beta) \langle \alpha || \delta T_{\Lambda} || \beta \rangle, \quad \dots 5$$

$$\langle \alpha || \delta T_{\Lambda} || \beta \rangle = \langle \alpha || T_{\Lambda} \frac{Q}{e_i - H_0} V_{res} || \beta \rangle +$$

$$\langle \alpha || V_{res} T_{\Lambda} \frac{Q}{e_f - H_0} T_{\Lambda} || \beta \rangle \quad \dots 6$$

where  $Q$  is the projection operator that projects the model space onto it.  $\alpha, \beta$  are single-particle between the initial and final state.

The Bohr-Mottelson (B.M) formula for the effective charge as follows<sup>18,19,20</sup>:

$$e^{eff}(t_z) = e(t_z) + e\delta e(t_z) \quad \dots 7$$

$$\text{Where, } \delta e(t_z) = Z/A - 0.32(N - Z)/A - 2t_z [0.32 - 0.3(N - Z)/A] \quad \dots 8$$

The electric quadrupole moment is given by<sup>14</sup>

$$Q(J = 2) = \begin{pmatrix} J_i & J & J_i \\ -J_i & 0 & J_i \end{pmatrix} \sqrt{\frac{16\pi}{5}} \langle J || \hat{E}(E2) || J \rangle \quad \dots 9$$

The  $B(E2)$  electric transition rate (reduced electric transition probability) can be defined as shown by Ref. <sup>15</sup>

$$B(E2) = \frac{Z^2}{4\pi} \frac{J}{J+1} \left[ \frac{(2J+1)!!}{k^J} \right]^2 \left| F_J^L(k) \right|^2 \quad \dots 10$$

Where  $k = \frac{E_x}{\hbar c}$ , is the long-wavelength limit the momentum transfer and  $E_x$  is the excitation energy. The deformation parameter ( $\beta_2$ ) is describes the quadruple deformation is given by <sup>9</sup>

$$\beta_2 = \frac{4\pi}{3ZR_0^2} \left[ \frac{B(E2)}{e^2} \right]^{\frac{1}{2}} \quad \dots 11$$

Where  $e$  is denote the electric charge of the proton,  $Z$  is the atomic number, and  $R_0 = 1.2$  fm. The average occupations number in each subshell  $j$  is given by:

$$occ\#(j, t_z) = OBDM(i, f, t_z, J = 0) \sqrt{\frac{2j+1}{2J_i+1}} \quad \dots 12$$

the mean root square radius  $\langle r^2 \rangle_\lambda$  for proton, neutron, and for matter is defined as <sup>14</sup>:

$$\langle r^2 \rangle_\lambda = \frac{1}{\lambda} \sum occ\# b^2 (N + \frac{3}{2}) \quad \dots 13$$

where  $N$  represents the total number of oscillator quanta excited, and  $\lambda$  represents the proton, neutron, and mass number.

The mean square charge radius is given by <sup>21</sup>:

$$\langle r_c^2 \rangle = \langle r_p^2 \rangle + 0.769 - \frac{N}{Z} 0.1161 + 0.033 \quad \dots 14$$

The radius of a nucleus's point proton dispersion is  $r_p$ , 0.769 is the charge radii of free proton and -0.1161 is the charge radii of free neutron, and the 0.033 terms is so-called Darwin–Foldy term.

## Results and Discussion:

The investigation of the electromagnetic properties of nuclei that are far from staying stable becomes one of the most important goals in nuclear physics. The calculations in this paper are done in fp model space with valence (active) neutrons in the

fp-shell. Calculations of the shell model are adopted using OXBASH code<sup>13</sup> to calculate the single-particle wave functions of the harmonic oscillator (HO) and using FPBM interaction by the one body matrix elements (OBME). The harmonic oscillator potential with size parameters  $b$  of some Ca isotopes are calculated by <sup>21</sup>

$$b = \sqrt{\frac{\hbar}{M_p \omega}}, \quad \text{where } \hbar\omega = 45A^{-1/3} - 25A^{-2/3} \quad \dots 15$$

( $M_p$  = mass of a proton).

## Occupation numbers (occ#)

The nuclear structure depends on the occ# is re-presenting the contribution of nucleons in each  $j$  state. In other words, all nuclear quantities depend on the distribution and contribution of nucleons in each state. From the shell model, the Ca isotopes are consisting of the core <sup>40</sup>Ca, and some valence nucleons outside the core in  $1f_{7/2}$ ,  $2p_{3/2}$ ,  $1f_{5/2}$  and  $2p_{1/2}$  orbits. The average number of nucleons in each  $j$ -level outside the core is shown in the Table.1. It's apparent that the highest ratio of this neutron's occupation numbers is  $1f_{7/2}$ . The occupation numbers percentages for all <sup>42,44,46,48,50</sup>Ca isotopes are calculated and shown in Fig. 1-A, B, C, D, E, respectively. The state  $1f_{7/2}$  is purely dominated when all valence nucleons occupy the state. The average of occ# increase for each state with the increases of the valence nucleons outside the core.

**Table 1. The occupation numbers (occ#) for the ground states of nucleons outside the core <sup>40</sup>Ca of considered for <sup>42, 44, 46, 48, 50</sup>Ca isotopes.**

Nucleus	Average no. of particles in each $j$ -level			
	$1f_{7/2}$	$2p_{3/2}$	$1f_{5/2}$	$2p_{1/2}$
<sup>42</sup> <sub>20</sub> Ca <sub>22</sub>	1.7980	0.1052	0.0763	0.0205
<sup>44</sup> <sub>20</sub> Ca <sub>24</sub>	3.6315	0.1709	0.1581	0.0395
<sup>46</sup> <sub>20</sub> Ca <sub>26</sub>	5.5224	0.2065	0.2139	0.0572
<sup>48</sup> <sub>20</sub> Ca <sub>28</sub>	7.5160	0.1981	0.2162	0.0697
<sup>50</sup> <sub>20</sub> Ca <sub>30</sub>	7.6011	1.4005	0.2569	0.7415

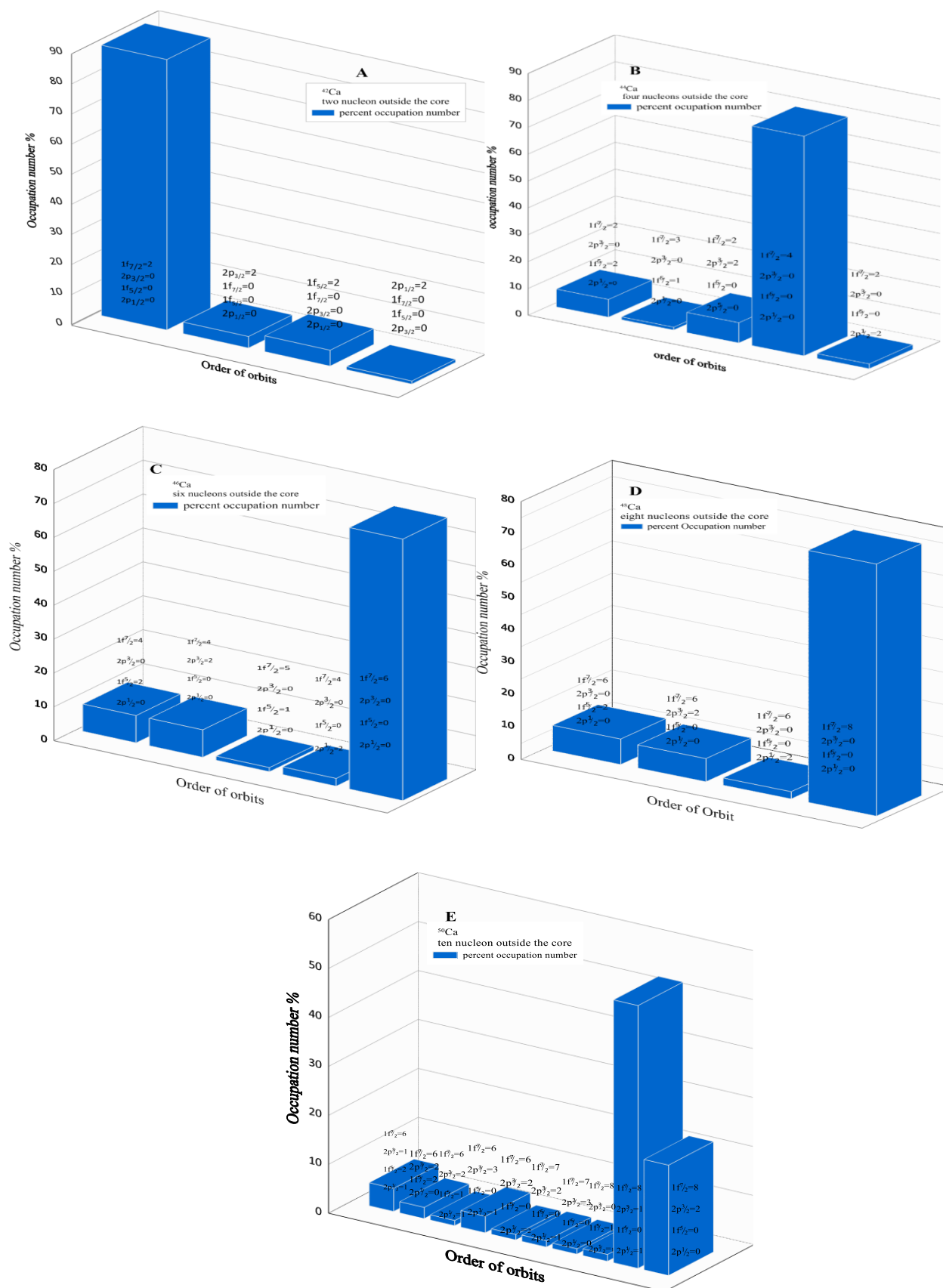


Figure 1. The occupation numbers percentage for the ground states of <sup>42,44,46,48,50</sup>Ca isotopes.

**Root-mean square-radius (rms)**

The available measured rms of proton, neutron, matter, and charge radii and the root-mean square-

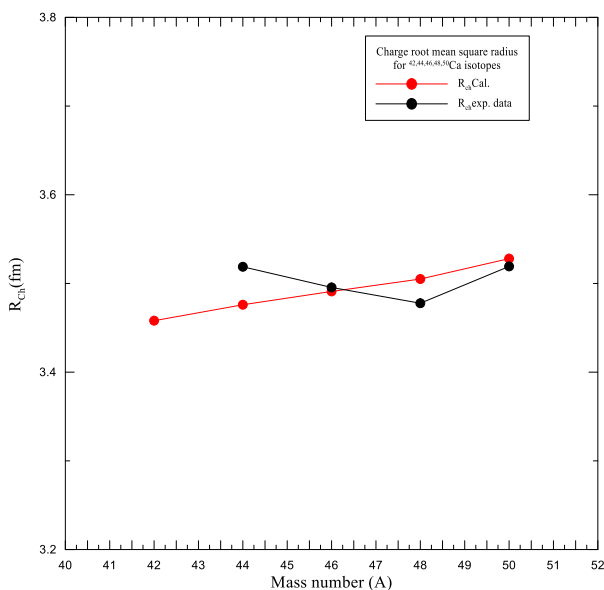
radius difference is called the neutron skin (is defined as the radial difference of the neutron and proton distributions with the surface thickness

( $R_\tau$ ), of calcium isotopes with,  $^{42}\text{Ca}(2^+1)$ ,  $^{44}\text{Ca}(2^+2)$ ,  $^{46}\text{Ca}(2^+3)$ ,  $^{48}\text{Ca}(2^+4)$ , and  $^{50}\text{Ca}(2^+5)$  are shown in Table.2. It was noticed that the value of rms increases with the increase of the size parameters of the nucleus, which in turn is directly proportional to the nucleus mass number Fig. 2. It's clear that the rms of proton, neutron, and matter

depend on the average value of occ# in each j-state and  $R_{ch}$  depends on radius of point proton distribution of a nucleus. The calculated  $R_{ch}$  are reproducing the experimental value <sup>22</sup> with the error. It is noticeable that the thickness of the skin for Ca isotopes increases with increasing numbers of valence neutrons.

**Table 2. The rms of proton, neutron, matter and charge radii and size parameters of the HO potential for  $^{42,44,46,48,50}\text{Ca}$  isotopes using FPBM interaction.**

Nucleus	J <sup>π</sup> T	b(fm)	R <sub>p</sub>	R <sub>n</sub>	R <sub>m</sub>	$R_\tau = R_n - R_p$	R <sub>ch</sub> Cal.	R <sub>ch</sub> exp. <sup>22</sup>
$^{42}_{20}\text{Ca}_{22}$	2 <sup>+</sup> 1	1.953	3.383	3.459	3.423	0.076	3.458	---
$^{44}_{20}\text{Ca}_{24}$	2 <sup>+</sup> 2	1.966	3.405	3.544	3.482	0.139	3.476	3.5188(21)
$^{46}_{20}\text{Ca}_{26}$	2 <sup>+</sup> 3	1.978	3.426	3.618	3.536	0.192	3.491	3.4955(23)
$^{48}_{20}\text{Ca}_{28}$	2 <sup>+</sup> 4	1.989	3.445	3.683	3.586	0.238	3.505	3.4777(25)
$^{50}_{20}\text{Ca}_{30}$	2 <sup>+</sup> 5	2.00	3.464	3.742	3.633	0.278	3.528	3.5192(26)



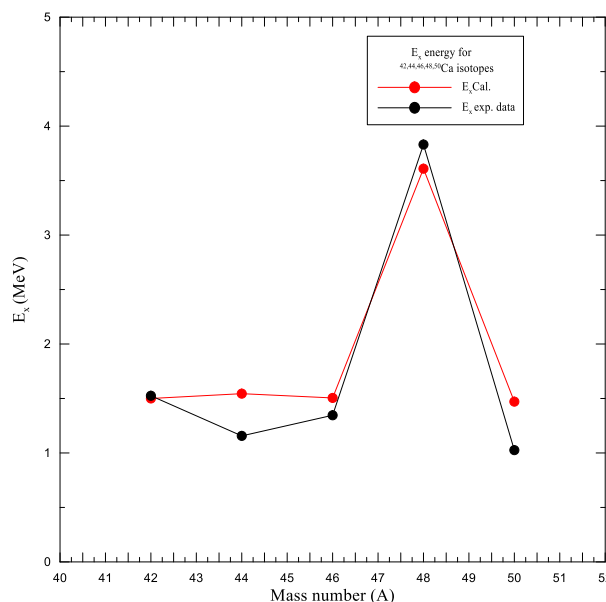
**Figure 2. Comparison between the calculated charge root mean square radius (red line) and experimental (black line) for  $^{42,44,46,48,50}\text{Ca}$  isotopes.**

Fig. 2 represents the comparison between the calculated charge root mean square radius (black line) and experimental charge root mean square radius (red line) <sup>22</sup> for  $^{42,44,46,48,50}\text{Ca}$  isotopes. From Fig. 2, we notice the convergence of the theoretical and experimental data with the presence of the error rate and that the theoretical values are identical to the experimental data at the mass numbers 46 and 50.

#### Excited energy level ( $E_x$ )

The excited energy level for transition ( $J_i = 0^+$  to  $J_f = 2^+$ ) for all  $^{42,44,46,48,50}\text{Ca}$  isotopes are calculated and compared to the results of experiment <sup>9</sup> are shown in Fig.3 and Table.4. The calculated excited energy fine agree with the experimental data at all mass number except at A=44 it underestimate the predicted by 1.33 factor. The

largest energy value is at  $A = 48$  because the valence nucleons are in the closed double subshell.



**Figure 3. Comparison between the calculated excited energy (black line) and experimental (red line) for  $^{42,44,46,48,50}\text{Ca}$  isotopes.**

#### Quadrupole moments ( $Q$ )

One of the most important factors for studying nuclear structure is the calculation of the nuclear electric quadrupole moments, which describes the effective shape of the ellipse for the distribution of nuclear charge within the nucleus. The shape of the nucleus depends on the values of the quadrupole moments, as its oblate for  $Q < 0$  and prolate for  $Q > 0$ .

The calculations are presented for Ca isotopes with even  $A=42$  to 50. These calculations include CP using MSDI theory and B.M formula effective charges. The results for  $Q$  moments are presented in table.3 and Fig.4 in comparison with the available experimental data of Ref. <sup>23</sup> and with the available

other theoretical results<sup>24</sup>. The results for  $Q$  moments of  $^{42}\text{Ca}$  are  $-1.576 e \text{ fm}^2$  and  $-1.306 e \text{ fm}^2$  calculated with effective charges, for proton and neutron  $e_p=1.634e$ ,  $e_n=0.634e$  and  $e_p=1.155e$ ,  $e_n=0.766e$  for CP and B.M, respectively. These values are in agreement with each other and underestimate the experimental value  $-19.0(8)^{23} e \text{ fm}^2$  by about a factor of 12.6 but with the same sign.

The theoretical quadrupole moment with CP effective charges  $e_p=1.634e$ ,  $e_n=0.634e$  for  $^{44}\text{Ca}$  is equal  $-4.616 e \text{ fm}^2$ , and the  $Q_{B.M}$  with effective charges  $e_p=1.443e$ ,  $e_n=0.443e$  is  $-7.481 e \text{ fm}^2$  which increases the discrepancy with the experimental  $-14.0(7)^{23} e \text{ fm}^2$  and theoretical value  $-6.4 e \text{ fm}^2$  but with a the same sign.

The calculated  $Q$  value for  $^{46}\text{Ca}$  with CP effective charges  $e_p=1.413e$ ,  $e_n=0.413e$  is  $-6.535 e \text{ fm}^2$  underestimate the calculated value with using the B.M effective charges  $e_p=1.112e$ ,  $e_n=0.674e$  is  $-10.25 e \text{ fm}^2$ . The  $Q_{B.M}$  result agrees with the theoretical value of Ref.<sup>24</sup>  $-10.4 e \text{ fm}^2$ . The present results cannot be compared with the quadrupole

experimental value because we do not have experimental values so we need more search.

The  $Q$  moments for  $^{48}\text{Ca}$  isotope (this isotope has two close sub-shell with neutron=28 magic numbers) with CP effective charges  $e_p=1.441e$ ,  $e_n=0.441e$  is  $3.18 e \text{ fm}^2$  underestimate the theoretical value  $4.0 e \text{ fm}^2$ <sup>24</sup>. This contradiction is solved by using the effective charges with B.M formula with  $e_p=1.093e$ ,  $e_n=0.633e$  is given  $Q$  equal to  $4.566 e \text{ fm}^2$ . This value agrees with the theoretical value  $4.0 e \text{ fm}^2$  of Ref.<sup>24</sup>.

The calculated  $Q$  moments for  $^{50}\text{Ca}$  isotopes with CP effective charges  $e_p=1.041e$ ,  $e_n=0.041e$  is  $-6.517 e \text{ fm}^2$  have underestimate the calculated  $Q$  using the B.M effective charges  $e_p=1.076e$ ,  $e_n=0.716e$  is  $-9.379 e \text{ fm}^2$ . These effective charges increase the value of  $Q$  by about once half times. There is no experimental value to compare with the present results.

The comparison between the experimental and calculated electric quadrupole moments for  $^{42,44,46,48,50}\text{Ca}$  isotopes is displayed in Fig. 4.

**Table 3. Calculated  $Q$  moments for  $^{42,44,46,48,50}\text{Ca}$  isotopes using FPBM interaction in comparison with available experimental<sup>23</sup> and other theoretical values<sup>24</sup>. Effective charges presented are deduced from CP using MSDI theory and with B.M formula.**

Nucleus	$J^\pi T$	$e_p, e_n$ C.P effective charge	$Q_{Theory}$ ( $e \text{ fm}^2$ )	$e_p, e_n$ (B.M) effective charge	$Q_{B.M.}$ ( $e \text{ fm}^2$ )	$Q_{exp.}$ ( $e \text{ fm}^2$ ) <sup>23</sup>	$Q_{Theory}$ Other results ( $e \text{ fm}^2$ ) <sup>24</sup>
$^{42}_{20}\text{Ca}_{22}$	$2^+ 1$	1.634,0.634	-1.576	1.155,0.766	-1.306	-19.0(8)	4.4
$^{44}_{20}\text{Ca}_{24}$	$2^+ 2$	1.443,0.443	-4.616	1.132,0.718	-7.481	-14.0(7)	-6.4
$^{46}_{20}\text{Ca}_{26}$	$2^+ 3$	1.413,0.413	-6.535	1.112,0.674	-10.25	-----	-10.4
$^{48}_{20}\text{Ca}_{28}$	$2^+ 4$	1.441,0.441	3.18	1.093,0.633	4.566	-----	4.0
$^{50}_{20}\text{Ca}_{30}$	$2^+ 5$	1.041,0.041	-6.517	1.076,0.716	-9.379	-----	-----

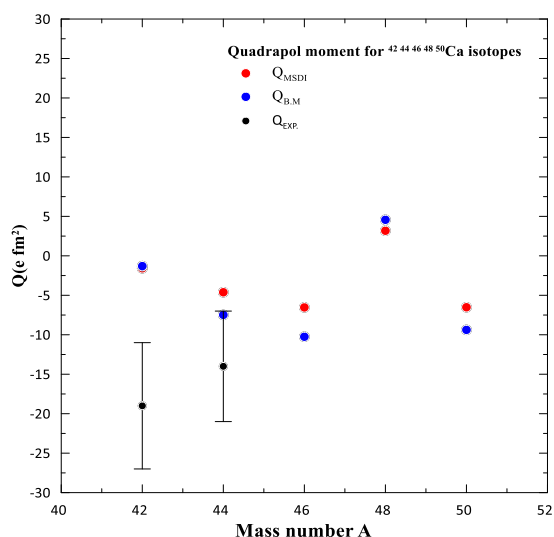


**Figure 4. The quadrupole moments for  $^{42,44,46,48,50}\text{Ca}$  isotopes. The experimental data (black circle) comparison with that calculated value using CP effective charges (red circle) and with using B.M formula (blue circle).**

### Reduced electric transition probability $B(E2)\uparrow$

A reduced transition probability,  $B(E2;0^+ \rightarrow 2^+)$ , is also calculated to investigate nuclear structure for  $^{42,44,46,48,50}\text{Ca}$  isotopes. The calculations of  $B(E2)\uparrow$  include effective charges by using the B.M formula. The results for  $B(E2)\uparrow$  are presented in Table (4) and Fig. 5 in comparison with the available experimental data of Ref.<sup>9</sup>. The calculated values of  $B(E2)\uparrow$  for  $^{42,44,46}\text{Ca}$  isotopes are less than the experimental values even if the error was added to the experimental values. This discrepancy between the calculated and experimental values of  $B(E2)\uparrow$  is due to the different distribution of nucleons in the sub-shell and to the effect of the core nucleons, while we note that the value of  $B(E2)\uparrow$  in the  $^{48}\text{Ca}$  kernel almost agree with the experimental values after adding the error. The value of  $B(E2)\uparrow$  in the  $^{50}\text{Ca}$  nucleus remains higher than the experimental value even after the addition of the error. Fig. 5 shows that the relation between the mass number and reduced transition probability,

the theoretical values approach the practical values with an increasing neutron or mass number.

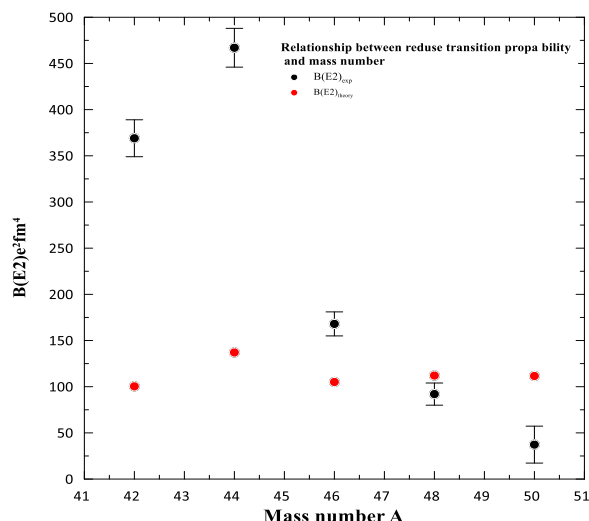


Figure 5. reduced transition probability for  $^{42,44,46,48,50}\text{Ca}$  isotopes. The experimental data (black circle) are comparison with that calculated value using B.M formula effective charges (red circle).

### Deformation parameter $\beta_2$

The deformation parameter  $\beta_2$  is defined as a measure of the deviation from the spherical shape of the nuclear charge distribution. The values of  $\beta_2$  depend on quadrupole moments and reduce transition probability. The calculated results of  $\beta_2$  are shown in Table.4 . For  $^{42,44,46}\text{Ca}$  isotopes, the results of  $\beta_2$  less than the experimental values<sup>9</sup>, while for  $^{48,50}\text{Ca}$  are a little higher than the experimental values. Fig.6 shows the mass number against the deformation parameter  $\beta_2$ , the theoretical values approach the practical values with an increasing mass number. Fig.7 shows the relation between  $\beta_2$  and  $B(E2)\uparrow$ . The relationship between them is direct.

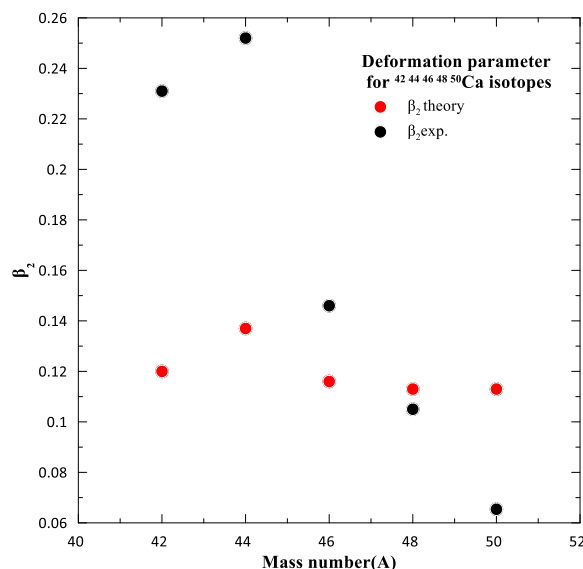


Figure 6. Deformation parameter for  $^{42,44,46,48,50}\text{Ca}$  isotopes. The experimental data (black circle) are comparison with that calculated value (red circle).

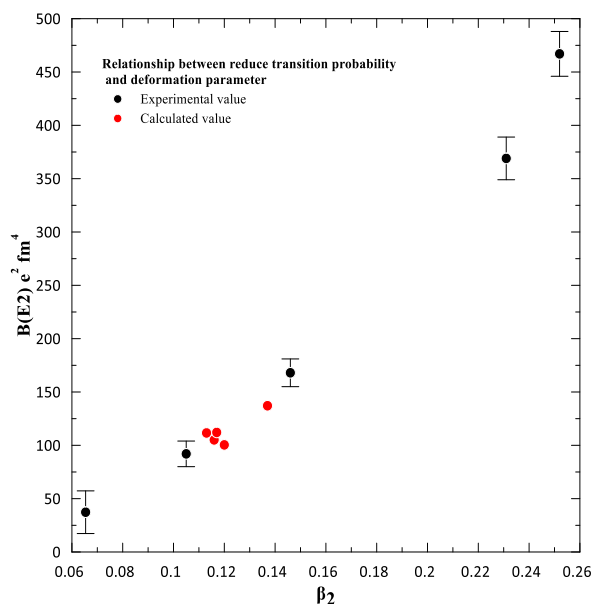


Figure7. Relation between the Deformation parameter and transition probability for  $^{42,44,46,48,50}\text{Ca}$  isotopes. The experimental data (black circle) are comparison with that calculated value (red circle).

Table 4. Calculated reduced electric transition probability  $B(E2)$  and deformation parameter  $\beta_2$  for  $^{42,44,46,48,50}\text{Ca}$  isotopes using FPBM interaction in comparison with available experimental data<sup>9</sup>.

Nucleus	$J^\pi T$	$E_{cal}(MeV)$	$E_{exp.}(MeV)$	$B(E2)_{cal.}\uparrow(e^2fm^4)$	$B(E2)_{exp.}\uparrow(e^2fm^4)^9$	$\beta_{2cal.}$	$\beta_{2exp}^9$
$^{42}_{20}\text{Ca}_{22}$	$2^+1$	1.5	1.525	100.4	369(20)	0.120	0.231(62)
$^{44}_{20}\text{Ca}_{24}$	$2^+2$	1.544	1.157	137.1	467(21)	0.137	0.252(57)
$^{46}_{20}\text{Ca}$	$2^+3$	1.505	1.346	105.1	168(13)	0.116	0.146(58)
$^{48}_{20}\text{Ca}_{28}$	$2^+4$	3.609	3.831	112.1	$92^{(+12)}_{(-5)}$	0.117	$0.105^{(+70)}_{(-29)}$
$^{50}_{20}\text{Ca}_{30}$	$2^+5$	1.471	1.026	111.6	$37.3^{(+20)}_{(-18)}$	0.113	$0.065^{(+18)}_{(-16)}$

### Inelastic longitudinal form factors

Electromagnetic properties can be determined the nuclear structure through the form factors. In

present results, the stable and exotic (neutron-rich) of some Ca isotopes are investigated through inelastic longitudinal electron scattering ( $0^+ \rightarrow 2^+$ ).

Fp-shell model with mixed configuration is adopted using FBPM interactions with the core of  $^{40}\text{Ca}$  plus (A- 20) residual nucleons divided over  $1f_{7/2}$ ,  $2p_{3/2}$ ,  $1f_{5/2}$ , and  $2p_{1/2}$  orbits, respectively. The  $C2$  longitudinal multipole form factors for  $^{42}\text{Ca}$  state with  $J^\pi T = 2^+ 1$  are shown in Fig.8-A. The results represent the model space + core polarization in comparison with that including the experimental data are taken from Ref. <sup>25</sup>. The red curve represents the calculation with CP using MSDI theory with calculation while the black curve represents the CP using effective charges with B.M formula with  $e_p = 1.155e$  and  $e_n = 0.7661e$ . The calculation form

factors have given a good description in general, but underestimate the experimental data at whole values of momentum transfer.

The  $C2$  components form factors of inelastic scattering for  $^{44}\text{Ca}$  with  $J^\pi T = 2^+ 2$  for calculated energy level (1.544 MeV) compared with experimental data of Ref. <sup>25</sup> are shown in Fig.8-B. The results of MS+CP using the MSDI theory (red curve) underestimate the experimental data at whole values of momentum transfer. Using B.M effective charges to calculated the core polarization with  $e_p = 1.132e$  and  $e_n = 0.718e$  (black curve) decreased these discrepancies especially at high q-value.

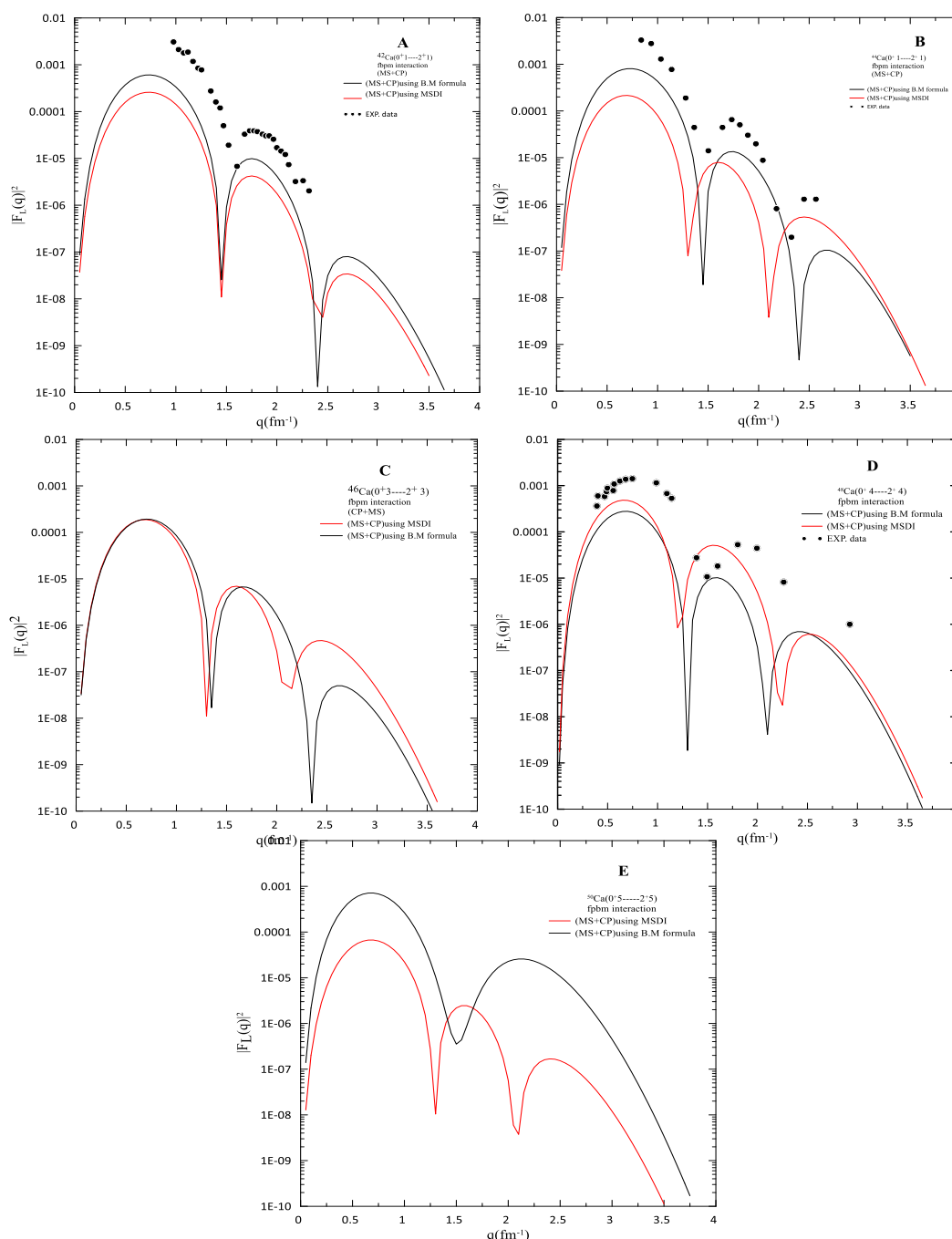


Figure 8. longitudinal inelastic form factors  $2^+$  for  $^{42,44,46,48,50}\text{Ca}$  isotopes.

The longitudinal form factors for the first excited state  $2^+ 3$  states of  $^{46}\text{Ca}$  nucleus with size parameter  $b=1.978\text{fm}$  are shown in Fig.8-C. There is no experimental data to compare with it. The calculated MS+CP using the B.M effective charges (black curve)  $e_p = 1.112 e$ ,  $e_n = 0.674 e$  close with the results MS+CP using the MSDI theory (red curve) at  $q < 1.6 \text{fm}^{-1}$ . The two results have the same behaviors but at the diffraction minimum.

Including the core polarization to the model space, the form factors of inelastic scattering for  $^{48}\text{Ca}$  with  $J^\pi T = 2^+ 4$  are calculated and shown in Fig.8-D. The results B.M effective charges (black curve) agree with the experimental data<sup>26</sup> with  $1.3 \leq q \leq 1.7 \text{fm}^{-1}$  while the calculate form factor with CP using MSDI theory underestimates experimental data at the all-region of momentum transfer.

The  $C_2$  components form factors of inelastic scattering for  $^{50}\text{Ca}$  with  $J^\pi T = 2^+ 5$  for calculated energy level (1.471MeV) and size parameter  $b= 2.0\text{fm}$  are shown in Fig.8-E. Unfortunately, there are no practical values for comparison with it. The results MS+CP using the MSDI theory (red curve) have two diffraction minimums at  $q=1.25$ , and  $q=2.1 \text{fm}^{-1}$  while the results using the B.M effective charges (black curve)  $e_p = 1.076e$ ,  $e_n = 0.716e$  have one diffraction minimum at  $q=1.5\text{fm}^{-1}$ , because of the exotic behavior for  $^{50}\text{Ca}$  nucleus.

### Conclusions:

In this work, we have investigated the nuclear structure of some Ca isotopes by calculating some electromagnetic properties using FPBM interaction. By analysis, the occupation numbers result strong contribution of  $1f_{7/2}$  orbit, and strange behavior is evident especially for neutron-rich isotopes. The rms of proton, neutron, matter and the excited energy level depend on the average value of  $\text{occ}\#$  in each j-state and  $R_{\text{ch}}$  depends on the radius of point proton distribution of a nucleus and the thickness of the skin for Ca isotopes increases with increasing numbers of valence neutrons. Calculations of reduced transition probability and deformation parameter  $\beta_2$  with B.M effective charge are better results, especially for neutron-rich isotopes. Including the CP by using microscopic theory and effective charges using B.M formula improves the values of the form factors and electric quadrupole moments. The B.M model gives better agreement with the predicted value and other theoretical values than that of the CP value.

### Authors' declaration:

- Conflicts of Interest: None.

- We hereby confirm that all the Figures and Tables in the manuscript are mine ours. Besides, the Figures and images, which are not mine ours, have been given the permission for republication attached with the manuscript.
- Ethical Clearance: The project was approved by the local ethical committee in University of Baghdad.

### Authors' contributions statement:

B. S. H. and T. A. A. are in visualizing and designing the study, obtaining data, in addition to analyzing and interpreting the results and writing the manuscript.

### References:

1. Suda T. Electron Scattering for Exotic Nuclei. J Phys Conf Ser. 2020 ;1643: 012159.
2. Brown BA, Garnsworthy AB, Kibedi T , Stuchbery AE. Microscopic method for E0 transition matrix elements. Phys Rev C. 2017; 95: 011301(R).
3. Ali AH. Study of the Electric Quadrupole Moments for some Scandium Isotopes Using Shell Model Calculations with Different Interactions. Baghdad Sci J.2019; 15(3): 304–309.
4. Garcia RF, Bissell ML, Blaum K, Frommgen N, Hammen M, Holt JD, et al. Ground-state electromagnetic moments of calcium isotopes. Phys Rev C. 2015; 91: 041304(R).
5. Ali AH, Hassoon SO, Tafash HT. Calculations of Quadrupole Deformation Parameters for Nuclei in fp shell. J Phys Conf Ser. 2019; 1178: 012010.
6. Hernández B, Sarriguren P, Moreno O, Moya de Guerra E, Kadrev D N, Antonov AN. Nuclear shape transitions and elastic magnetic electron scattering. Phys Rev C. 2021; 103: 014303.
7. Ali AH, Hameed BS. Calculation the Magnetic Dipole Moments and Quadrupole Moments for Some Exotic Chromium Isotopes Using Different Interactions. Rom J Phys. 2020; 65: 305.
8. Radhi RA, Alzubadi AA, Manie SM. Electromagnetic multipoles of positive parity states in  $^{27}\text{Al}$  by elastic and inelastic electron scattering. Nucl Phys A. 2021; 1015: 122302.
9. Pritychenkoa B, Birchb M, Singhb B, Horoi M. Tables of E2 Transition Probabilities from the first  $2^+$  States in Even-Even Nuclei. At. Data Nucl. Data Tables. 2016; 107: 1- 139.
10. Pritychenko B, Birch M, Singh B. Revisiting Grodzins Systematics of B(E2) values. Nucl Phys A. 2017; 962(16): 73-102.
11. Skyy VP, Kristian K, Dominic M R, Brown BA, Inorvati A, Lantis J, et al. Charge Radius of Neutron- deficient  $^{54}\text{Ni}$  and Symmetry Energy Constraints Using the Difference in Mirror Pair Charge Radii. Phys Rev Lett. 2021; 127: 182503.

12. Richter WA, Van der Merwe MG, Julies RE, Brown BA. New effective interactions for the  $0f_{7/2}$  shell. Nucl Phys A. 1991; 523: 325-353.
13. Brown BA, Etchegoyen A, Godwin NS, Rae WD M, Richter W A, Ormand W E, et al. MSU-NSCL report number. 2005; 1289.
14. Brussaard PJ, Glademans PWM. Shell-model Application in Nuclear Spectroscopy. North-Holland Publishing Company, 1<sup>st</sup> Ed. Amsterdam. 1977; 452.
15. Brown BA, Wildenthal BH, Williamson CF, Rad FN, Kowalski S, Crannell H, et al. Shell-model analysis of high-resolution data for elastic and inelastic electron scattering on  $^{19}\text{F}$ . Phys Rev C. 1985; 32: 1127.
16. Tassie LJ, Barker FC. Application to Electron Scattering of Center-of-Mass Effects in the Nuclear Shell Model. Phys Rev. 1958; 111: 940.
17. Glickman JP, Bertozzi W, Buti TN, Dixit S, Hersman FW, Hyde-Wright C E, et al. Electron Scattering from  $^9\text{Be}$ . Phys Rev C. 1991; 43: 1740.
18. Bohr A, Mottelson BR. Nuclear Structure. 1<sup>st</sup> Ed. Benjamin, New York. 1969; 2 : 515.
19. Radhi RA, Alzubadi AA, Ali AH. Magnetic dipole moments, electric quadrupole moments, and electron scattering form factors of neutron-rich  $sd$ - $pf$  cross-shell nuclei. Phys Rev C. 2018; 97(6): 1–13.
20. Ali AH. Investigation of the Quadrupole Moment and Form Factors of Some Ca Isotopes. Baghdad Sci J. 2020; 17(2): 502-508.
21. Brown BA, Radhi R, Wildenthal BH. Electric quadrupole and hexadecapole nuclear excitation from the perspectives of electron scattering and modern shell-model theory. Phys Rep. 1983; 101: 313.
22. Li T, Luo Y, Wang N. Compilation of recent nuclear ground state charge radius measurements and tests for models. At. Data Nucl Data Tables. 2021; 140: 101440.
23. Stone NJ. Table of nuclear electric quadrupole moments. IAEA Nuclear Data Section Vienna International Centre, INDC(NDS)-0833 Distr. ND.2021; 20.
24. Iwamoto T, Horie H. Inelastic electron scattering form factors for the excitation of the  $2^+$  states in the  $1f_{7/2}$  nuclei. Phys Rev C . 1982; 25: 658.
25. Heisenberg J, McCarthy JS, Sick I. Inelastic electron scattering from several Ca, Ti and Fe isotopes. Nucl Phys A. 1971; 164: 353-366.
26. Wise JE, McCarthy JS, Altemus R, Norum BE, Whitney RR, Heisenberg J, et al. Inelastic electron scattering from  $^{48}\text{Ca}$ . Phys Rev C . 1985; 31: 1699.

## دراسة التركيب النووي لبعض نظائر الكالسيوم الزوجية- زوجية باستخدام النظرية المجهرية

بان صباح حميد

تبارك عبد الله علوان

قسم الفيزياء، كلية العلوم للبنات، جامعة بغداد، بغداد، العراق.

### الخلاصة:

تم حساب جذر متوسط مربع نصف قطر للبروتون ، والنيوترون ، وأنصاف أقطار المادة والشحنة ، ومستوى الطاقة ، وعوامل التشكل الطولية غير المرنة ، واحتمالية الانتقال المنخفضة من الحالة الأرضية إلى الحالة المثارة الأولى  $2^+$  للنظائر الزوجية-زوجية والعزوم الرباعية و معاملات التشوه الرباعية وأعداد الأشغال لبعض نظائر الكالسيوم لـ  $A=42,44,46,48,50$  باستخدام نموذج الفضاء  $fp$  وتفاعل FPBM على اعتبار أن نواة  $^{40}\text{Ca}$  قلباً خاملاً لجميع النظائر المدروسة في فضاء هذا النموذج ، حيث تتحرك نيوكلونات التكافؤ في جميع أنحاء فضاء النموذج  $fp$  والتي تشتمل على مدارات  $2p_{1/2}$  و  $1f_{7/2}$ ,  $2p_{3/2}$ ,  $1f_{5/2}$  . يتم حالياً حساب فضاء النموذج باستخدام تفاعل FPBM، ومع تأثيرات استقطاب القلب يتم الحصول عليها من خلال استقطاب القلب من الرتبة الأولى من خلال النظرية المجهرية تفاعل سطح دلنا المعدل التي تسمح بإثارة جميع المدارات الأعلى عن طريق تهيج جسيم-فجوة من النواة ومدارات الفضاء النموذجية. كذلك تم تحديد الشحنات الفعالة لكل نظير باستخدام النموذج التجميعي بواسطة صيغة بور- موتلسون. النتائج الحالية تتوافق مع البيانات التجريبية من خلال مراعاة تأثيرات استقطاب القلب.

الكلمات المفتاحية: معاملات التشوه، عامل التشكل، أعداد الأشغال، والعزوم الرباعية، احتمالية الانتقال.